

## Supporting Information

# A-site composition tuning in methylammonium- based metal halide perovskite colloidal nanocrystals

Shekhar Mondal,<sup>a,b</sup> Gauri Sharma,<sup>b,c</sup> Sunanda Bhoi,<sup>a</sup>, Sadashiv Wadepalli,<sup>a,b</sup> Pralay K. Santra,<sup>b,c</sup> Dipankar Saha<sup>d</sup> and Abhijit Hazarika<sup>\*a,b</sup>

<sup>a</sup>*Polymers and Functional Materials Division,  
CSIR-Indian Institute of Chemical Technology, Uppal Road, Tarnaka, Hyderabad, 500007,  
India.*

<sup>b</sup>*Academy of Scientific and Innovative Research (AcSIR), Ghaziabad 201002, India.*

<sup>c</sup>*Centre for Nano and Soft Matter Sciences (CeNS), Bengaluru, India 562162;*

<sup>d</sup>*Department of Chemistry, University of Oslo, Blindern 0315 Oslo*

\*Corresponding author email: [abhijit@iict.res.in](mailto:abhijit@iict.res.in)

**Synthesis of Cs-oleate precursor.** Cs-oleate precursor was prepared by taking 1.25 mmol (0.407 g) of Cs<sub>2</sub>CO<sub>3</sub>, 20 ml 1-ODE and 1.25 ml OA in a 3-necked round bottom flask under degassing condition at 60 °C for 45 minutes followed by heating at 150 °C under N<sub>2</sub> atmosphere. Once the clear solution formed the Cs-oleate was kept at 120 °C under N<sub>2</sub> atmosphere for further use.

**Synthesis of FA-oleate precursor.** FA-oleate was synthesized by following a reported method where 5 mmol (0.521 g) of FA-acetate and 10 ml OA were taken in a 3-necked round bottom flask and degassed at 50 °C for 30 minutes. Then the temperature of the reaction mixture was raised to 120 °C under N<sub>2</sub> atmosphere. Once a dark brown coloured clear solution was obtained the temperature was decreased to 80 °C and kept for injection.

**Synthesis of MA-oleate precursor.** 2.5 mmol (0.227 g) MA-acetate and 10 ml OA were loaded in a 3 necked round bottom flask and degassed at 50 °C for 1 hour followed by increasing the temperature to 80 °C under N<sub>2</sub> atmosphere. Once light brown colour clear solution was formed it was kept at 80 °C for further use.

**Synthesis of Oleylammonium Iodide salt.** 12.5 ml OIAm and 100 ml ethanol were loaded in a single necked RB and it was stirred vigorously in an ice bath. In this condition 10 ml HI (57 % aqueous solution) was added dropwise to the OIAm. The mixture was left to react overnight under ambient condition. Then the solution was dried under rotatory evaporator to obtain dark brown coloured product which was then recrystallized multiple times from diethyl ether. The final product was dark brown in colour.

#### **Calculation of Relative Band Gap Bleach.**

For the band gap bleach analysis of MAPI thin film, PNC film and TCPbI<sub>3</sub> film the relative band gap bleach with time was calculated for the respective films. The first order derivative of the absorption data was plotted and the peak at the first excitonic position was recorded. Now, from day 1 to day 7 we observed decrease in the peak intensity at the first excitonic position (near to band edge) for each film. To calculate the relative bandgap bleach, the peak intensity (derived from first order derivative of absorption data) corresponding to each day was divided by the peak intensity of the day 1 (which is maximum). Now, these relative intensities were plotted against time.

#### **Details of Rietveld Analysis.**

Rietveld refinements were carried using TOPAS 6.0 software out to establish the phases of the nanocrystals (Bruker-AXS, TOPAS 6.0, 2017, Karlsruhe). An instrumental parameter file was determined by profile fitting the Si NIST standard data and was included during the Rietveld refinements. Starting model of Rietveld refinement was chosen from the structure solved by neutron diffraction of Deuterated FAPI.<sup>1</sup> All peaks FAPI could be indexed in cubic structure with *Pm-3m* symmetry and lattice constant of 6.3613(8) Å, (*Pm-3m*). This confirms that FAPI

crystallizes in the cubic space group where Pb atoms occupy the centre of the cube and the iodine occupies the edge of the cube forming an octahedron. FA<sup>+</sup> cations have random orientation in the cubic phase. A rotating organic cation was placed around (0 0 0) position with dynamical averaging over time to satisfy the cubic symmetry. Occupancy and thermal parameters of FAPI were kept constant during the Rietveld Refinement. Atomic coordinates of Cubic phase of FAPI are listed in Table S1. The starting model for MAPI was chosen from single crystal data.<sup>2</sup> Only particle size was refined to limit the number of variable parameters. Stress and strain parameters were not refined during the Rietveld refinement. For the Solid solution of MAPI and FAPI, disordered MAPI was included around (0 0 0) position (Excluding Hydrogen Atom). Occupancies of carbon and nitrogen were adjusted according to the starting composition during synthesis.

Table S1: Fractional Coordinates of FAPI in the space group *Pm-3m*

	Atom	x	y	z	Occupancy	B eq
1	Pb1	0.5	0.5	0.5	1	5.276
2	I2	0.5	0	0.5	1	4.34
3	C1	-0.079	-0.014	-0.022	0.0208	2.29
4	H1	-0.206	-0.102	-0.009	0.0208	2.29
5	N2	-0.038	0.122	0.141	0.0208	2.29
6	H2A	0.078	0.206	0.136	0.0208	2.29
7	H2B	-0.126	0.127	0.254	0.0208	2.29
8	N3	0.040	-0.038	-0.201	0.0208	2.29
9	H3A	0.159	0.040	-0.218	0.0208	2.29
10	H3B	0.001	-0.133	-0.302	0.0208	2.29

Table S2: Fractional Coordinates of MAPI in the space group *Fmmm*

	Atom	x	y	z	Occ.	Beq.
1	Pb1	0.2500	0.2500	0.5000	1	4.548
2	I1	0.2241	0.5000	0.5000	1	4.46
3	I2A	0.5000	0.2981	0.5000	0.75	4.185
4	I2B	0.5000	0.2670	0.4620	0.125	4.185
5	I3A	0.2500	0.2500	0.2500	0.75	5.306
6	I3B	0.2940	0.2500	0.2500	0.125	5.306
7	C1	0.5000	0.4426	0.2160	0.5	2.84
8	N1	0.5000	0.4426	0.2160	0.5	2.84

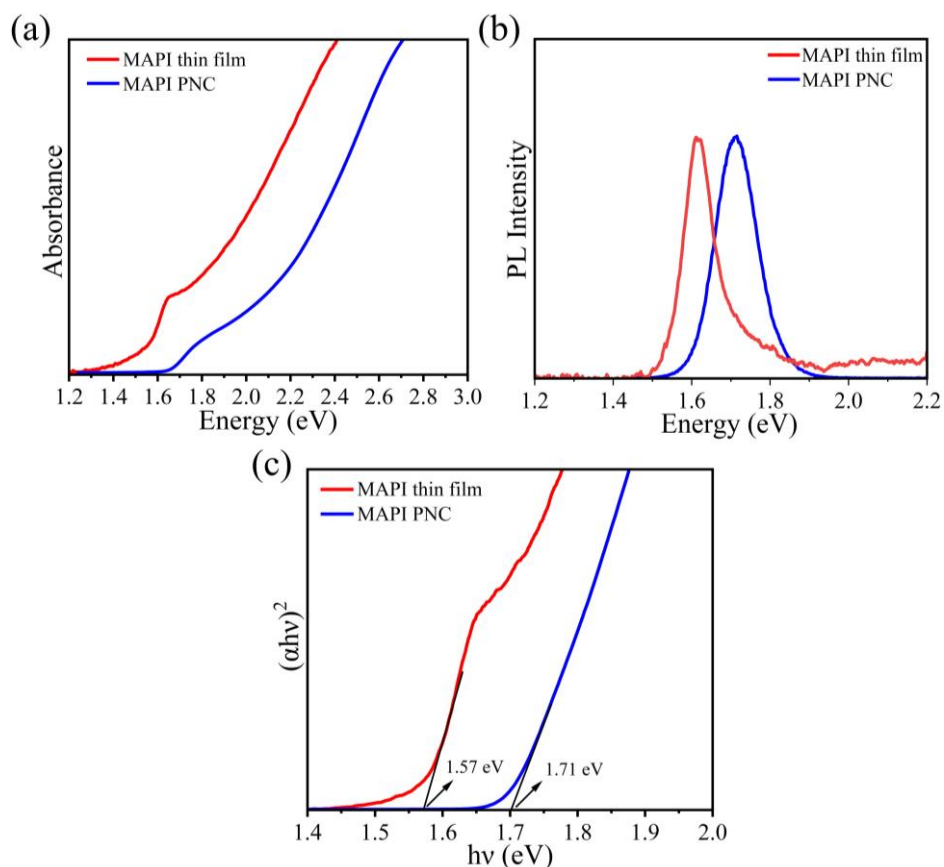


Figure S1: (a) UV-Vis absorption spectra and (b) PL emission spectra of  $\text{MAPbI}_3$  polycrystalline/ bulk film (MAPI-PC) and  $\text{MAPbI}_3$  PNCs (MAPI-PNC) colloidal solution, (c) Tauc plot of MAPI PC film and PNC obtained from their corresponding absorption spectra showing that the band gap of MAPI PNCs is blue shifted by  $\sim 0.14$  eV compared to the MAPI PC film.

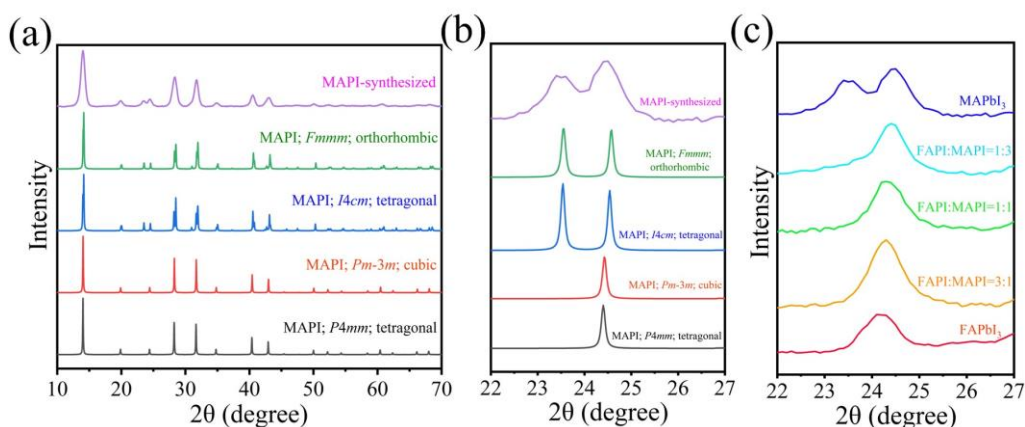


Figure S2: (a) Comparison of powder XRD of the synthesized  $\text{MAPbI}_3$  PNCs with standard reported bulk patterns,<sup>2-4</sup> (b) zoomed-in view of the XRD patterns from (a), (c) zoomed-in view of the XRD patterns of MAPI PNCs compared to other PNC compositions to show splitting of the peak at  $2\theta = 24.3^\circ$ .

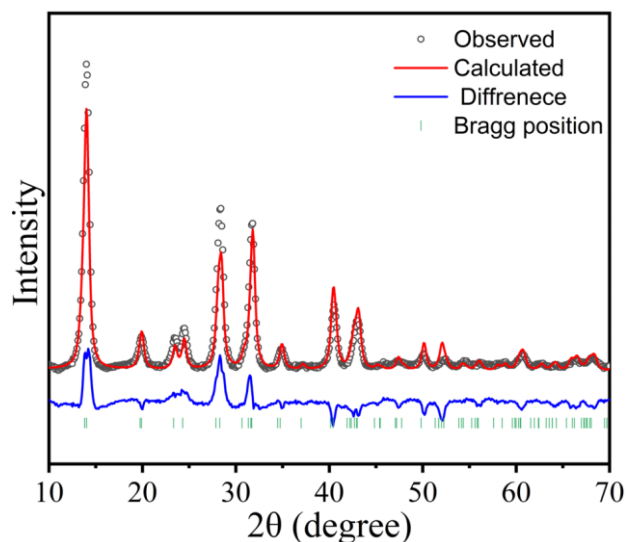


Figure S3: MAPI PXRD data fitted with tetragonal(I4cm) structure

Table S3: background corrected  $R_p$  and  $R_{wp}$  values for the fitted orthorhombic structure of MAPI PNCs.

	Without background subtracted	Background subtracted
$R_p$	10.17	18.45
$R_{wp}$	13.47	21.65

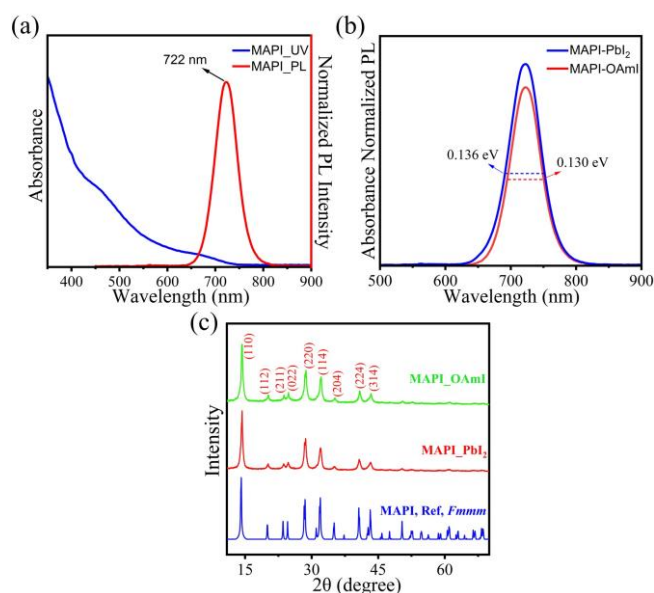


Figure S4: (a) UV-Vis absorption and PL emission spectra of the  $\text{MAPbI}_3$  PNCs synthesized via three precursors method (route II) using OAmI, (b) Comparison of absorbance normalized PL intensity of  $\text{MAPbI}_3$  PNCs synthesized via two precursor method using  $\text{PbI}_2$  (blue) and three precursors method using OAmI (red), (c) Powder XRD pattern of the  $\text{MAPbI}_3$  PNCs

synthesized via two different methods, the diffraction peaks for the MAPbI<sub>3</sub> PNCs were indexed following Stoumpos *et al.*<sup>3</sup>

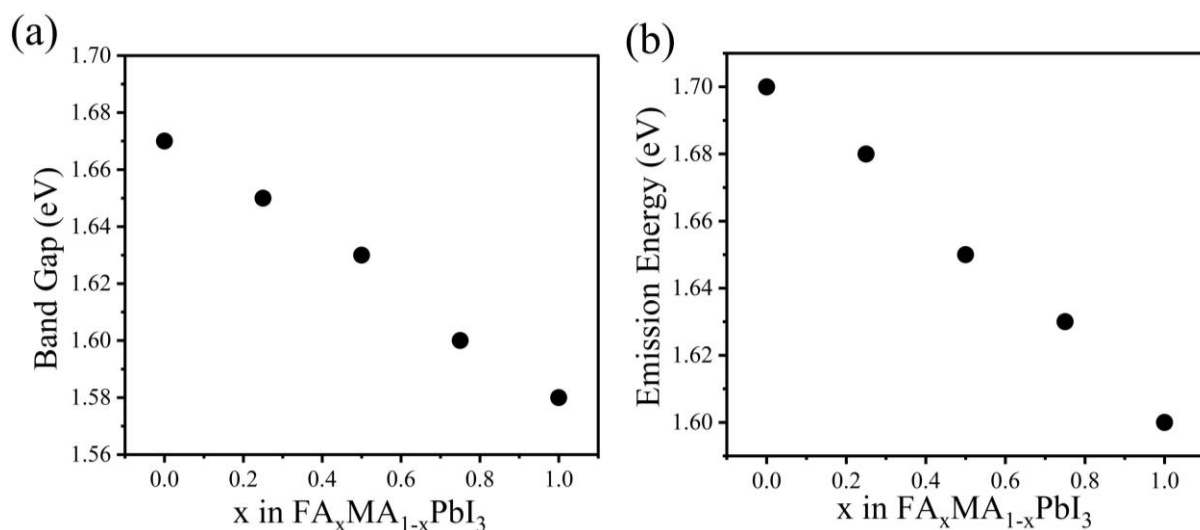


Figure S5: Linear variation of (a) band gap and (b) emission energies of FA<sub>x</sub>MA<sub>1-x</sub>PbI<sub>3</sub> solid solutions with the composition 'x'.

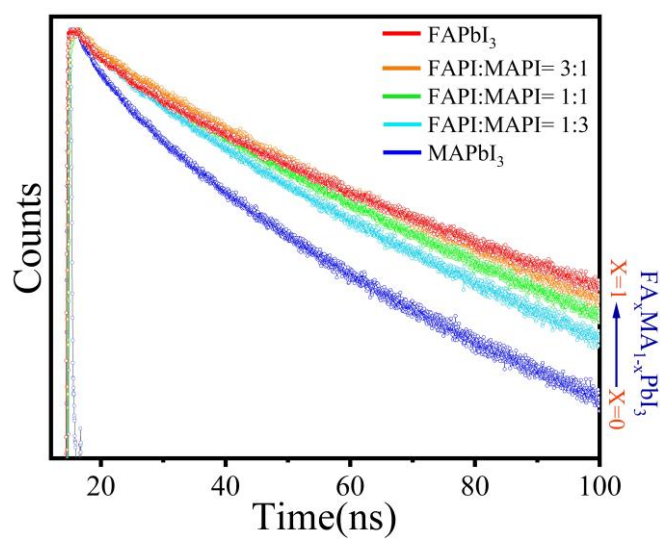


Figure S6: Time Resolve PL spectra (TRPL) of the PNCs solid solution showing faster PL decay with increasing MA content in the FA<sub>x</sub>MA<sub>1-x</sub>PbI<sub>3</sub>.

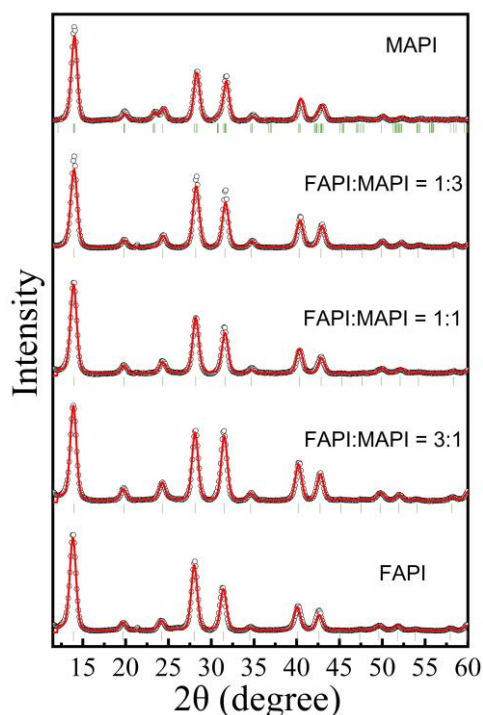


Figure S7: Rietveld fitted XRD pattern of the  $\text{FA}_x\text{MA}_{1-x}\text{PbI}_3$  compositions ( $x = 0$  to 1).

Table S4: Fitting parameters, calculated lattice parameters and cell volume obtained from Rietveld Refinement of the powder XRD pattern of  $\text{FA}_x\text{MA}_{1-x}\text{PbI}_3$  ( $x = 0$  to 1) solid solutions.

Composition ( $\text{FA}_x\text{MA}_{1-x}\text{PbI}_3$ )	$x = 1$	$x = 0.75$	$x = 0.5$	$x = 0.25$	$x = 0$
$R_p(\%)$	10.91	8.03	10.45	14.46	10.17
$R_{wp}(\%)$	14.77	11.22	14.09	18.30	13.47
$R_{exp}(\%)$	4.29	5.90	6.29	5.45	6.56
DWD	0.15	0.45	0.34	0.20	0.38
GOF	3.01	1.98	2.24	3.36	2.05
Space group	$Pm-3m$	$Pm-3m$	$Pm-3m$	$Pm-3m$	$Fmmm$
$a$ (Å)	6.3613(8)	6.3416(6)	6.3274(5)	6.326(10)	12.59(2)
$b$ (Å)					12.64(3)
$c$ (Å)					12.72(2)
Volume (Å <sup>3</sup> )	257.41(9)	255.04(8)	253.32(9)	253.2(13)	2023(6)
Reduced cell and volume in Cubic settings					6.317(3) 252.07(2)

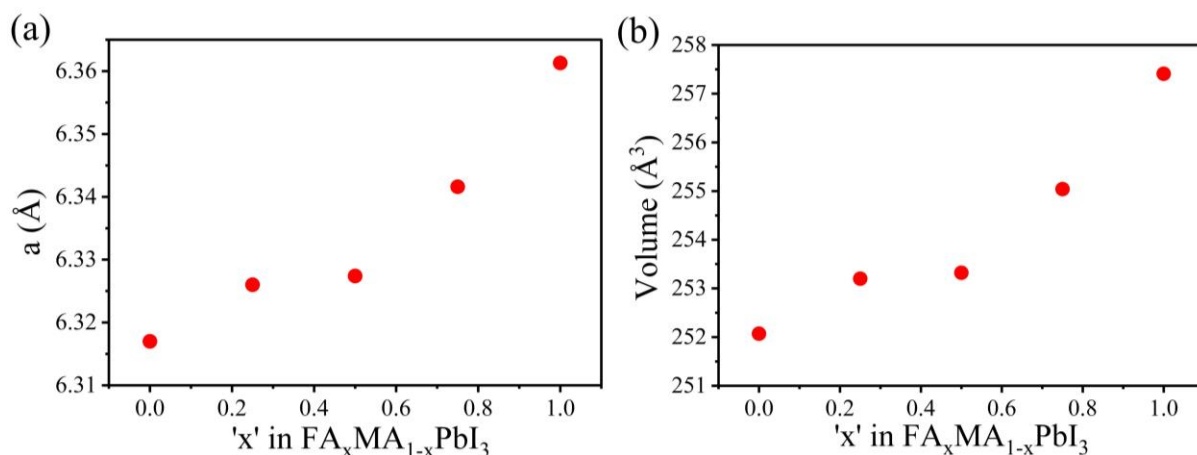


Figure S8: Variation of (a) lattice parameters and (b) cell volume with 'x' in  $\text{FA}_x\text{MA}_{1-x}\text{PbI}_3$  solid solutions.

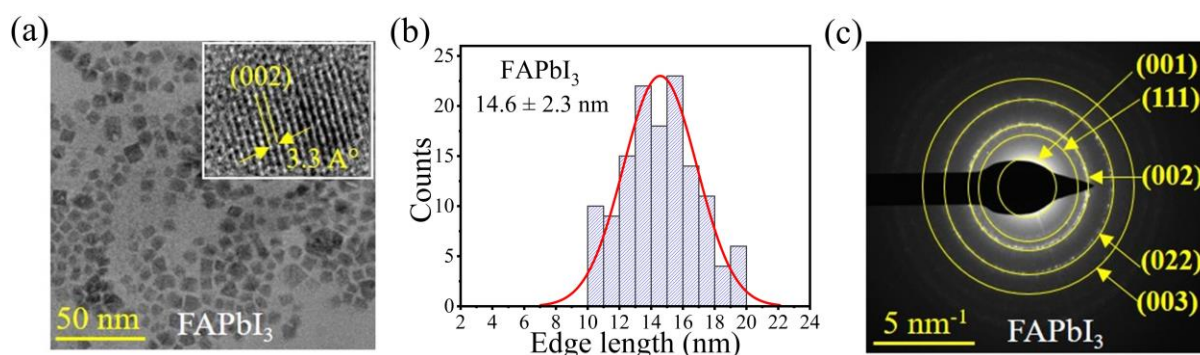


Figure S9: (a) TEM images of FAPI PNCs at 50 nm scale; the inset is showing zoomed in view of PNCs of cubic morphology, (b) TEM size distribution histogram of FAPI PNCs showing average edge length of  $14.6 \pm 2.3 \text{ nm}$ , (b) (c) SAED patterns of FAPI PNCs; the planes were assigned according to the d-spacing value calculated from powder XRD pattern.

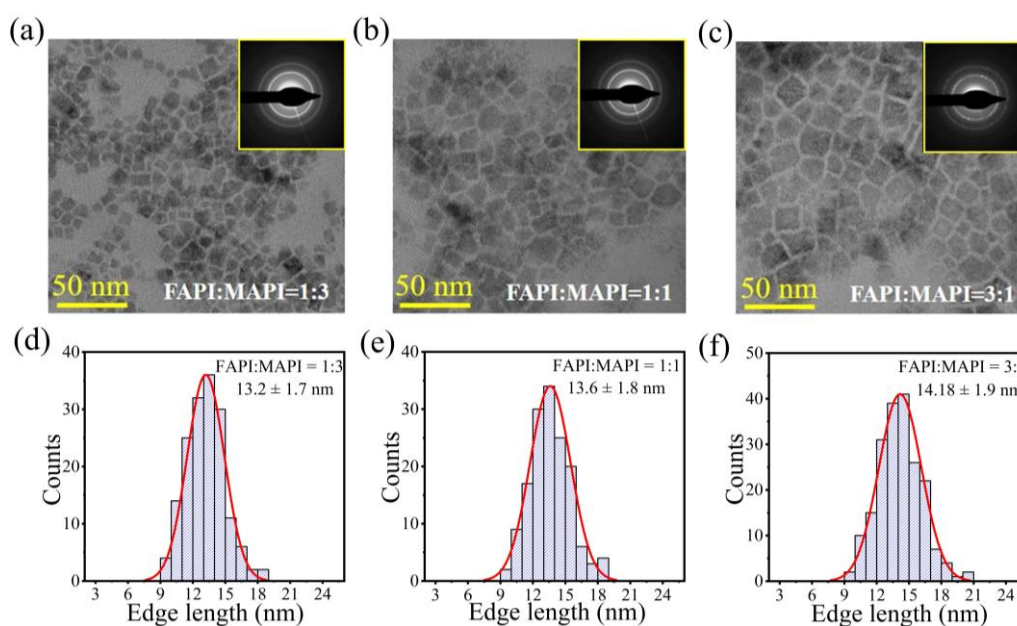




Figure S10: (a-c) TEM images of  $\text{FA}_x\text{MA}_{1-x}\text{PbI}_3$  solid solution (inset is showing the SAED pattern of the corresponding solution which prove the polycrystallinity of those PNCs solid solution) : (a) FAPI:MAPI = 1:3, (b) FAPI:MAPI = 1:1 and (c) FAPI:MAPI = 3:1, (d-f) Particle size distribution histogram of  $\text{FA}_x\text{MA}_{1-x}\text{PbI}_3$  alloy : (d) FAPI:MAPI = 1:3, (e) FAPI:MAPI = 1:1 and (f) FAPI:MAPI = 3:1.

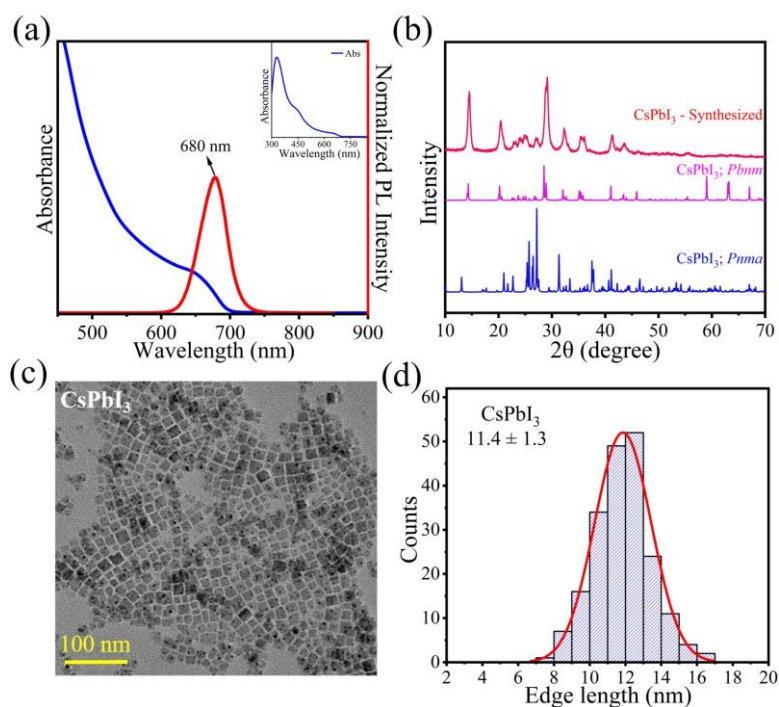


Figure S11: (a) UV-Vis absorption (blue) and PL emission (red) spectra of synthesized  $\text{CsPbI}_3$  PNCs; the inset is showing the complete absorption profile in the range of 300-800 nm, (b) Powder XRD pattern of synthesized  $\text{CsPbI}_3$  PNCs (red); comparison of the powder XRD pattern with the standard reference of space group  $Pbnm^5$  and  $Pnma^3$  is shown, (c) TEM images of  $\text{CsPbI}_3$  indicating that PNCs are forming in cubic morphology, (d) TEM -Histogram is showing that the  $\text{CsPbI}_3$  PNCs have average edge length of  $11.4 \pm 1.3$  nm.

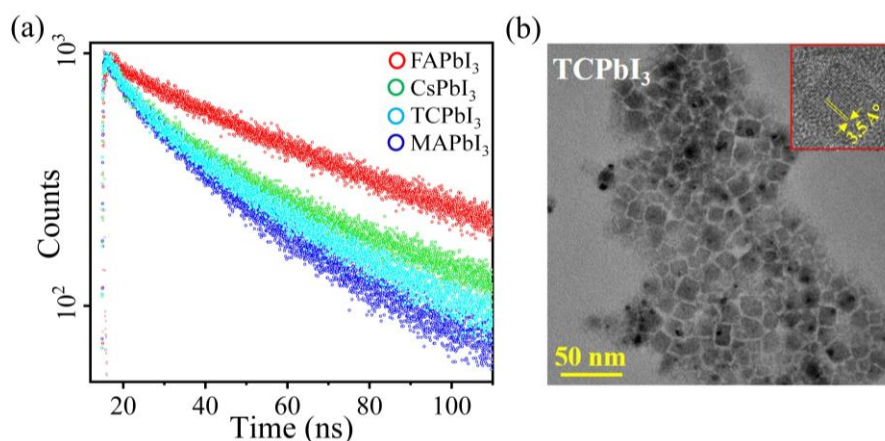


Figure S12: (a) Time Resolve PL spectra (TRPL) of the TCPbI<sub>3</sub> PNCs (CPI:MAPI:FAPi = 1:1:1) along with their parent PNCs, (b) TEM image of the same TCPbI<sub>3</sub> PNCs; showing the retention of cubic morphology similar to its parent counterpart.

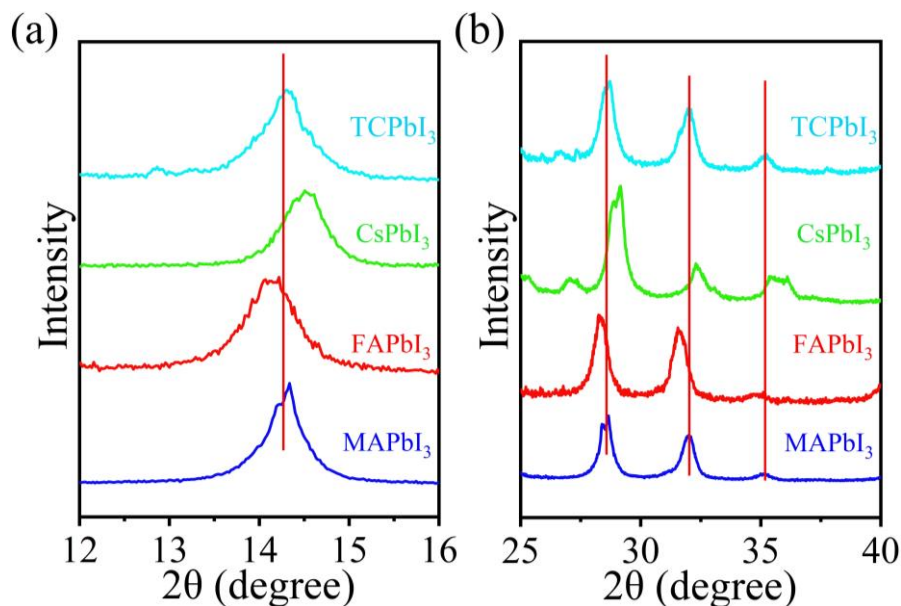


Figure S13: (a-b) Zoomed-in view of the powder XRD pattern of the TCPbI<sub>3</sub> PNCs (with CPI:MAPI:FAPi = 1:1:1) along with their parent PNCs.

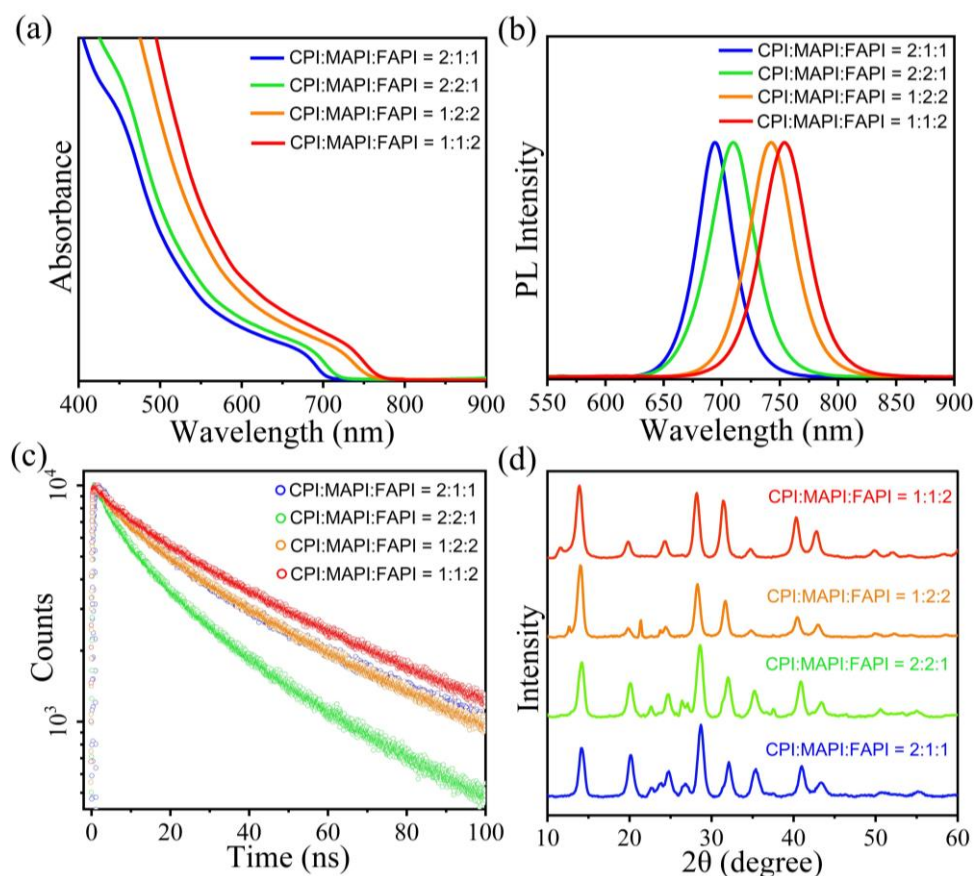


Figure S14: (a) UV-Vis absorption spectra (b) steady state PL emission spectra, (c) time resolved PL spectra and (d) powder XRD pattern of four different compositions of TCPbI<sub>3</sub> NCs.

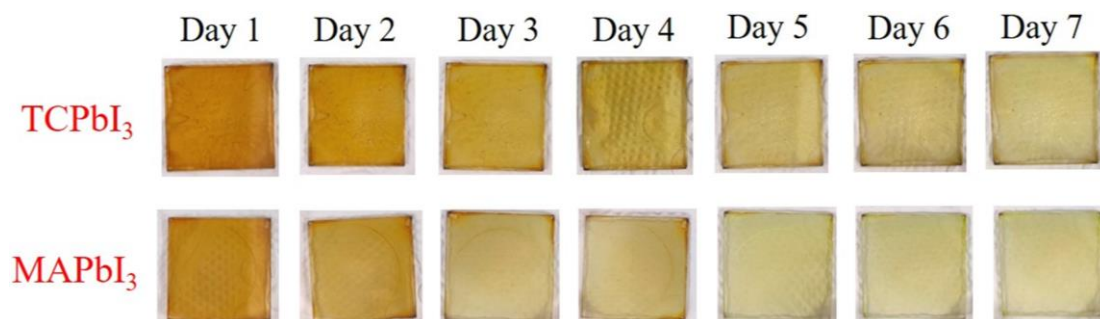


Figure S15: Digital photograph of MAPbI<sub>3</sub> and TCPbI<sub>3</sub> PNCs film showing how the colour of the film is changing with time; the films were kept in ambient atmosphere in 50-70% relative humidity (RH) under normal light and room temperature (25-30 °C).

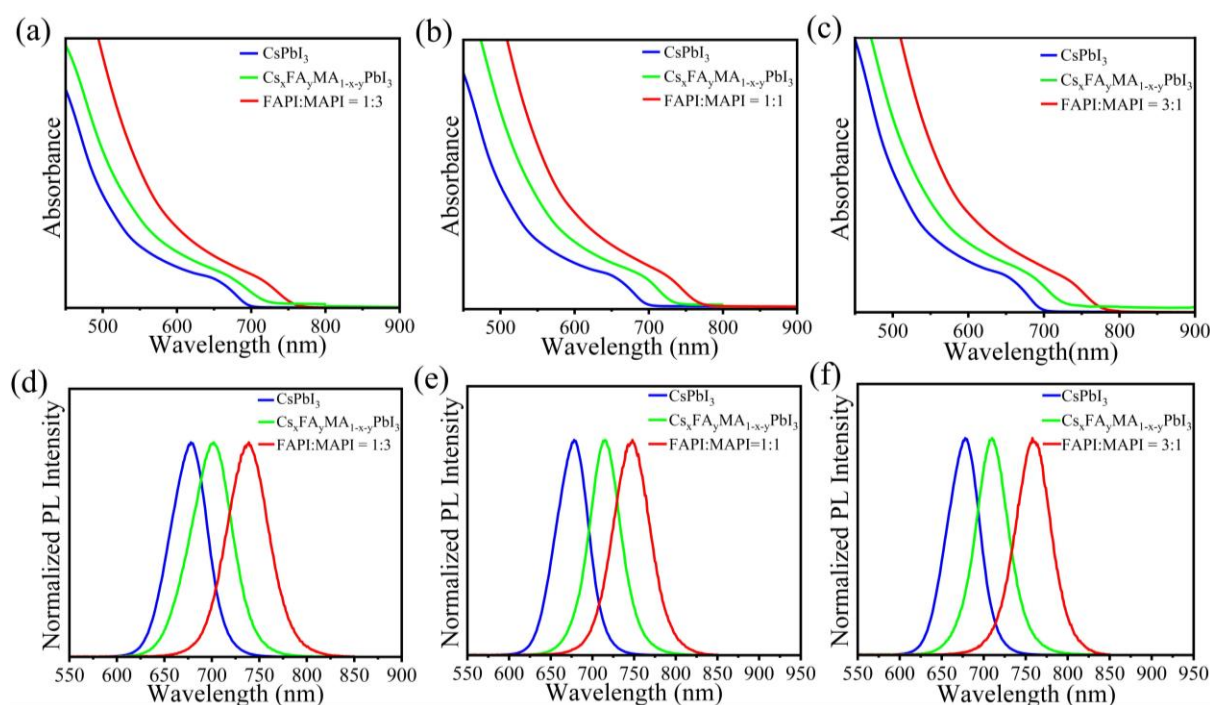


Figure S16: UV-Vis absorption spectra of TCPbI<sub>3</sub> prepared with (a) CsPbI<sub>3</sub> & FAPI:MAPI=1:3, (c) CsPbI<sub>3</sub> & FAPI:MAPI=1:1 & (e) CsPbI<sub>3</sub> & FAPI:MAPI=3:1 and PL emission spectra of TCPbI<sub>3</sub> prepared with (b) CsPbI<sub>3</sub> & FAPI:MAPI=1:3, (d)CsPbI<sub>3</sub> & FAPI:MAPI=1:1 & (f) CsPbI<sub>3</sub> & FAPI:MAPI=3:1.

## References

- (1) T. Chen, B.J. Foley, C. Park, C.M. Brown, L.W. Harriger, J. Lee, J. Ruff, M. Yoon, J.J. Choi, S.-H. Lee, *Sci. Adv.*, **2**, e1601650(2016).
- (2) A. Jaffe, Y. Lin, C.M. Beavers, J. Voss, W.L. Mao and H.I. Karunadasa, *ACS Cent. Sci.*, 2016, **2** (4), 201-209.
- (3) C.C. Stoumpos, C.D. Malliakas and M.G. Kanatzidis, *Inorg. Chem.*, 2013, **52** (15), 9019-9038.
- (4) P.S. Whitfield, N. Herron, W.E. Guise, K. Page, Y.Q. Cheng, I. Milas and M.K. Crawford, *Sci Rep*, 2016, **6** (1), 35685.
- (5) J.A. Vigil, A. Hazarika, J.M. Luther and M.F. Toney, *ACS Energy Lett.* 2020, **5** (8), 2475-2482.